

Enabling pulse compression and proton acceleration in a modular ICF driver for nuclear and particle physics applications

F. Terranova^a, S.V. Bulanov^{b,c}, J.L. Collier^d, H. Kiriya^b, F. Pegoraro^e

^a I.N.F.N., Laboratori Nazionali di Frascati, Frascati (Rome), Italy

^b Advanced Photon Research Centre, JAERI, Kizu-cho, Kyoto-fu, Japan

^c A. M. Prokhorov General Physics Institute of RAS, Moscow, Russia

^d Central Laser Facility, Rutherford Appleton Laboratory, Didcot, UK

^e Dip. di Fisica, Univ. di Pisa and CNISM, Pisa, Italy

Abstract

The existence of efficient ion acceleration regimes in collective laser-plasma interactions opens up the possibility to develop high-energy physics facilities in conjunction with projects for inertial confinement nuclear fusion (ICF) and neutron spallation sources. In this paper, we show that the pulse compression requests to make operative these acceleration mechanisms do not fall in contradiction with current technologies for high repetition rate ICF drivers. In particular, we discuss explicitly a solution that exploits optical parametric chirped pulse amplification and the intrinsic modularity of the lasers aimed at ICF.

1 Introduction

Particle acceleration through collective short wavelength electromagnetic effects has been pursued for decades [1]. The advent of laser has made it possible to use the interaction of the laser light with the charged particles [2] and the plasma [3] and this technique is still considered a viable alternative to traditional RF-based boosters. Such a confidence has been strengthened after the advent of wideband oscillators based on Ti:sapphire and the revolution in power ultrafast lasers due to the development of Chirped Pulse Amplification [4] (CPA). Production of energetic ions and electrons has been reported by several experimental groups and new breakthroughs are expected after the commissioning of the next generation of multi-petawatt lasers. Nonetheless, there is large consensus on the fact that a well-understood and stable regime of acceleration hasn't been achieved, yet. The lack of a reference mechanism is the root of the best known drawbacks of laser acceleration: strong dependence on the initial conditions, large energy spread, poor light-to-particle energy conversion efficiency and significant shot to shot variations. These limitations, however, are unlikely to be intrinsic features of laser acceleration. This is particularly clear for ion acceleration. It has long been understood that fast ion generation is related to the presence of hot electrons [5]. A variety of effects occur when the main source of acceleration is charge displacement due to the electron motion in the plasma or inductive electric fields from self generated magnetic fields [6]. However, for higher laser intensities (10^{23} W/cm²) acceleration results from the laser pressure exerted to the comoving electron-ion system; the latter acts as a progressively more opaque screen for the laser light and, in this case, charge displacement only plays the role of rectifier for the transversal laser field and as a medium for electron-ion energy transfer during light absorption. This mechanism is described in details in [7, 8, 9]. It provides energy transfer efficiency comparable to RF-based synchrotrons or even cyclotrons and, more importantly, decouples the final ion energy from the accelerated ion current (see Sec.4). If this mechanism were confirmed experimentally, it could represent the first serious alternative to synchrotrons suited for high energy physics (HEP) applications. As noted in [8], a proof of principle of this radiation-pressure dominated (RPD) acceleration mechanism is at the borderline of current technology, but the possibility of using this technique to overcome the limitations of traditional proton accelerators faces many additional difficulties. In particular all present high power lasers operate at very low repetition rate. This is a classical problem e.g. in inertial confinement fusion (ICF), where the basic principle could be demonstrated, for instance, at the National Ignition Facility (NIF) in US [10] on a single-shot basis. However, the ultimate use of ICF to produce electric power will require repetition rates of the order of tens of Hz, an increase of several order of magnitude compared to the shot rate achievable with state-of-the-art fusion laser technology. This rate cannot be achieved with flashlamp-pumped neodymium-doped glass lasers that requires a significant interpulse cooling time. There is, currently, a very large effort to find alternative solutions and promising setups based on excimer lasers or diode-pumped solid state lasers have been identified, offering, in principle, the repe-

tition rates needed for ICF. In [8], we noted that the solution of the problem of thermal stability and the exploitation of the RPD mechanism would open up the fascinating possibility of a multipurpose driver for ICF and HEP applications. However, we did not address explicitly the question whether the power requirements for ICF could fall in contrast with the pulse compression requests needed for the RPD acceleration to be fully operative. More precisely, the strong constraints on the choice of the amplifying medium (and therefore on the gain bandwidth) could make impossible an appropriate pulse compression, so that the intensity needed to operate in the RPD regime would not be reached by a multi-pulse device. In this paper we show that there exists at least one particular configuration that is able to fulfill simultaneously the two requirements; i.e. it offers a high repetition rate device that can be implemented to design a multi-GeV proton booster with a technology suited for ICF energy production. This solution is based on the exploitation of optical parametric chirped pulse amplification [11, 12] (OPCPA) and the intrinsic modularity of ICF drivers¹ (see Sec.2); it is described in details in Sec. 3, while its potentiality as a new generation proton driver is discussed in Sec. 4

2 Drivers for Inertial Confinement Fusion

Large scale flashlamp-pumped solid state lasers built for ICF are inherently single shot devices, requiring several hours to recover from thermal distortions. They are aimed at a proof-of-principle for ICF but their scaling to a cost effective fusion reactor is highly non trivial. In the last decade, three main research lines have been investigated and much more efforts will be put in the forecoming years if the proof-of-principle programs for ICF at NIF or at Laser Megajoule (LMJ) in France is successful. The first one exploits traditional RF-based technologies for ion acceleration to transfer energy to the target, trigger ignition and sustain burning. This approach profits of the enormous experience gained in particle accelerators since the 50's and the large efficiency ($\sim 30-35\%$) obtained at HEP facilities [13] but, as a matter of fact, the mean intensities and the required uniformity of target illumination are well beyond current technology. The second and third ones exploit lasers to ignite and sustain fusion and are aimed at developing systems with much higher thermal yield than Nd:glass. They are based on diode-pumped solid state lasers (DPSSL) or high power excimer lasers.

¹These drivers are constituted by an ensemble of independent beamlines. Synchronous operation of the beams is requested for fusion applications since the power must be delivered in a single shot (maximum peak power) and illuminate uniformly the fuel target. However, in most of the applications related to particle and nuclear physics, the performance of the facility mainly depends on the achieved mean power and asynchronous operation modes can be envisaged. This simplifies substantially the technological challenge of the feedback system for light synchronization.

2.1 Diode-pumped solid state lasers

The possibility of building ICF lasers with high repetition rates and efficiency using solid state materials mainly relies on the substitution of flashlamps with low-cost laser diode arrays and the development of crystals for greater energy storage and thermal conductivity than Nd:glass [14]. Yb:crystals cooled by near sonic helium jets are presently favorite candidates. The main advantage of this approach is that it retains most of the features of Nd:glass systems, first of all the possibility (still to be demonstrated) of $< 1\%$ smooth irradiation on-target for direct drive in a timescale of fractions of ns. A DPSSL-based fusion reactor would be - like NIF - highly modular. One possible vision is based on 4 kJ DPSSL composed of 1 kJ beamlets operating at a repetition rate of the order of 10 Hz and assembled to reach the overall MJ power per shot. To our knowledge, the most advanced R&D project is the Mercury/Venus laser system [15]. In particular, the Mercury R&D is aimed at a 100 J, 10 Hz laser based on gas cooled Yb:S-FAP crystals grown up to 20 cm diameter [16]. The laser operates at 1047 nm (1ω) with a 2 ns pulsewidth, a 5x diffraction limited beam quality and an efficiency greater than 5%. Fusion drivers are better operated at higher frequencies to increase the rocket efficiency and reduce laser-plasma instabilities [17]. Hence, DPSSL are operated at 3ω (349 nm) with a conversion efficiency greater than 80%. Gain bandwidth is of the order of 5 nm for Yb:S-FAP, significantly lower than for Nd:glass (28 nm) so that the time duration of a DPSSL Fourier-limited (chirp-free) TEM_{00} output beam would be bandwidth limited to ~ 0.3 ps pulses.

2.2 Excimer lasers

Excimer power lasers have been developed both for laser fusion and defense uses. The current main candidate for ICF is krypton-fluoride. Electron beam pumped KrF systems offer superior beam spatial uniformity, short wavelength and high laser efficiency ($\sim 10\%$). As for DPSSL, an excimer-based fusion reactor is highly modular and single beamlines could provide up to 50 kJ of laser light [17]. Again, the thermal yield and the efficiencies requested for a viable commercial power plant [18] represent major technological challenges. The laser operates at 248 nm but a certain degree of tunability is offered by the fact that the same system design can be re-used for other gas mixtures [19] (e.g. ArXe lasing at 1733 nm or XeF at 351 nm). In particular, XeF has been the leading candidate for defense applications and large aperture lasers with energy yield per pulse in the 5 kJ range has been built since the late 80's [20]. XeF has also been considered for laser fusion but it is less effective than KrF due to its lower efficiency and because it behaves spectrally inhomogeneous, precluding efficient narrow-band operation [21].

3 OPCPA pulse compression

As a by-product of its peculiar design (see Sec.2), a multi-shot ICF driver offers a large number of beamlines operating, probably, in the near-UV region with a rather limited spectral bandwidth and an energy per pulse ranging from 1 to 50 kJ. We do not expect a Ti:sapphire CPA system being able to use efficiently neither this pump source nor its outstanding average power regime. On the other hand, Optical Parametric Chirped Pulse Amplification offers, in principle, a higher degree of tunability and could be successfully adapted to exploit a narrow band, energetic pump pulse [22] and its average power [23]. Pulse compression should be enough to trigger the RPD acceleration mechanism and exploit the high repetition rate to increase the average ion current². Optical parametric amplification is a nonlinear process that involves a signal wave, a pump and an idler wave [24]. In a suitable nonlinear crystal, the high intensity and high frequency pump beam (ω_p) amplifies a lower frequency (ω_s), lower intensity signal. Energy conservation is fulfilled through the generation of a third beam (“idler”) whose frequency is constrained by

$$\omega_p = \omega_s + \omega_i. \quad (1)$$

Parametric gain is achieved over the coherence length, defined as the length over which the phase relationship among the three waves departs from the ideal condition (“phase matching”). Phase matching corresponds to momentum conservation and can be expressed as

$$\vec{k}_p = \vec{k}_s + \vec{k}_i, \quad (2)$$

\vec{k}_p , \vec{k}_s , \vec{k}_i being the wave vectors of pump, signal and idler, respectively. Clearly, energy and momentum conservation cannot be fulfilled simultaneously in a linear crystal but birefringence offers a way out. In spite of the variety of nonlinear crystals developed so far for frequency multiplication, only a few can be grown to large size (tens of cm) to handle the pump energy available and offer an adequate fluence limit for high power applications. Here, we mainly concentrate on Potassium Dihydrogen Phosphate (KDP), a negative uniaxial crystal commonly used for frequency multiplication of Nd:YAG lasers³. In this case, phase matching can be achieved for parallel beams

²We do not intend this technique as a route for Fast Ignition since the spectrum of the ions is too energetic once the RPD regime is operational.

³In the rest of the paper we assume for KDP the following Sellmeier’s equations:

$$n_0^2 = 2.259276 + \frac{0.01008956}{\lambda^2 - 0.012942625} + 13.00522 \frac{\lambda^2}{\lambda^2 - 400} \quad (3)$$

for the ordinary index and

$$n_e^2 = 2.132668 + \frac{0.008637494}{\lambda^2 - 0.012281043} + 3.2279924 \frac{\lambda^2}{\lambda^2 - 400} \quad (4)$$

for the principal extraordinary index (λ is the wavelength in μm). The nonlinear coefficients are $d_{36} \simeq d_{14} = 0.44$ pm/V.

(“collinear geometry”) when the pump beam is at an angle θ_m with respect to the KDP optical axis:

$$n_{ep}(\theta_m)\omega_p = n_{os}\omega_s + n_{oi}\omega_i. \quad (5)$$

Note that in the present configuration the pump beam is polarized along the extraordinary direction, while both the signal and the idler beam have ordinary polarization (“Type I” phase matching). Recalling

$$n_{ep}^{-2}(\theta_m) = \sin^2(\theta_m)n_{ep}^{-2} + \cos^2(\theta_m)n_{op}^{-2} \quad (6)$$

n_{ep} and n_{op} being the principal extraordinary and ordinary refractive indexes at pump wavelength, we get:

$$\theta_m = \text{asin} \left[\frac{n_{ep}}{n_{ep}(\theta_m)} \sqrt{\frac{n_{op}^2 - n_{ep}^2(\theta_m)}{n_{op}^2 - n_{ep}^2}} \right]. \quad (7)$$

It is worth mentioning that θ_m shows a less pronounced dependence on the wavelength for Type I phase matching than for type II, i.e. the case when only the idler or the signal has ordinary polarization [25]. This is an additional advantage when broad amplification bandwidth is sought for.

Fig.1 shows the FWHM amplification bandwidth for a KDP-based Type I amplifier operated in collinear geometry. The bandwidth has been computed assuming a pump wavelength of 349 nm (see Sec.2) and a pump intensity of 2 GW/cm². The latter is determined by the fluence F at which the crystal is operated and the pump pulse duration τ . Following [12], we assumed here $F=1.0$ J/cm² for KDP and $\tau=0.5$ ns⁴. The gain bandwidth has been computed assuming no pump depletion so that the gain G can be approximated as [12, 26]

$$G = 1 + (\Gamma L)^2 \left[\frac{\sinh B}{B} \right]^2 \quad (8)$$

where $B \equiv [(\Gamma L)^2 - (\Delta k L/2)^2]^{1/2}$; Γ represents the gain coefficient

$$\Gamma \equiv 4\pi d_{eff} \sqrt{\frac{I_p}{2\epsilon_0 n_{ep}(\theta_m) n_{os} n_{oi} c \lambda_s \lambda_i}}; \quad (9)$$

the quantity L is the length of the crystal and $\Delta k \equiv k_p - k_s - k_i$ is the phase mismatch among signal, idler and pump. Note that in collinear geometry, this quantity is scalar since the wave vectors lay along the same axis. d_{eff} is the effective nonlinear coefficient: for Type I phase matching in KDP

$$d_{eff} = -d_{14} \sin \theta \sin 2\phi \quad (10)$$

⁴In fact, KDP can be operated at higher fluencies since its optical damage threshold is greater than 5 GW/cm² but no long-term reliability studies are available for these extreme values. Note also that competing nonlinear processes like self-focusing or self-phase modulations have been neglected.

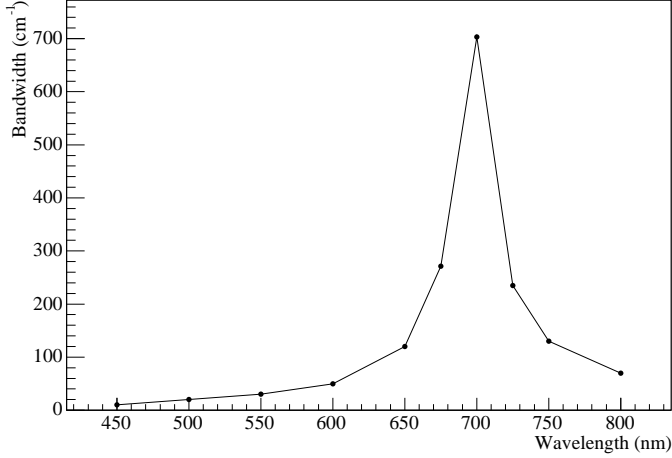


Figure 1: FWHM bandwidth expressed in wavenumbers ($1/\lambda$) versus signal wavelength for $\lambda_p = 349$ nm. The KDP-based amplifier ($G=1000$ at central wavelength) is operated in Type I collinear mode (see text for details).

where θ is the angle between the propagation vector and the optic axis and ϕ is the azimuthal angle between the propagation vector and the xz crystalline plane⁵. Hence, $\theta = \theta_m$ and ϕ can be chosen to maximize d_{eff} ($\phi = \pi/4$). In Fig.1, as well as in Ref. [12], L has been equalized in order to attain $G = 1000$. In particular, for $\lambda_s = 700$ nm, such a gain is reached at $L = 2$ cm.

Fig.1 points toward the existence of a window for full exploitation of the original pump power. More precisely, a faint, chirped, wideband seed signal could be amplified by a chain of Type I amplifiers [27] and finally enter the power KDP-based amplifier depleting the intense pump wave⁶. However, a significant improvement in bandwidth can be achieved operating the system in non-collinear mode. In this case the pump and signal wave vectors are no more parallel but form an angle α between them (Fig.2). The angle is independent of the signal wavelength. Again, the idler frequency is fixed by energy conservation but the emission angle Ω varies with λ_s . Therefore, the matching conditions become

$$\Delta k_{||} = k_p \cos \alpha - k_s - k_i \cos \Omega = 0 \quad (11)$$

$$\Delta k_{\perp} = k_p \sin \alpha - k_i \sin \Omega = 0 \quad (12)$$

The additional degree of freedom coming from the introduction of α can be exploited to improve the gain bandwidth. In particular, it helps achieving phase matching at first order for small deviations from the central signal wavelength. It corresponds to

⁵For the axis notation see [24].

⁶A complete numerical analysis of the signal evolution in pump depletion mode is beyond the scope of this paper. A full calculation for Nd:glass pumps has been carried out in [27].

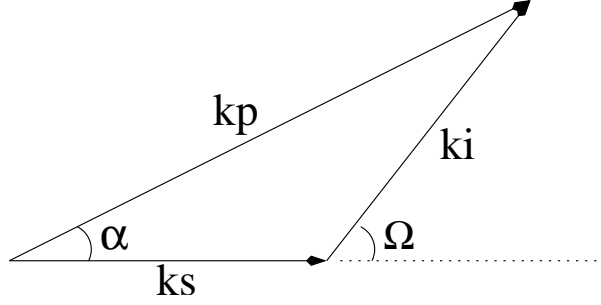


Figure 2: Phase matching triangle for noncollinear OPCPA.

imposing [25]

$$\left. \frac{d\Delta k_{\parallel}}{d\omega} \right|_{\omega=\omega_s} = 0 \quad (13)$$

$$\left. \frac{d\Delta k_{\perp}}{d\omega} \right|_{\omega=\omega_s} = 0 \quad (14)$$

together with the energy conservation constraint (i.e. a finite increase $\Delta\omega$ of the signal frequency corresponds to a finite decrease $-\Delta\omega$ of the idler).

Eqs.13 and 14 are equivalent to:

$$-\frac{dk_s}{d\omega_s} + \frac{dk_i}{d\omega_i} \cos \Omega - k_i \sin \Omega \frac{d\Omega}{d\omega_i} = 0 \quad (15)$$

$$-\frac{dk_i}{d\omega_i} \sin \Omega + k_i \cos \Omega \frac{d\Omega}{d\omega_i} = 0 \quad (16)$$

and are simultaneously fulfilled if

$$\frac{dk_i}{d\omega_i} - \cos \Omega \frac{dk_s}{d\omega_s} = 0. \quad (17)$$

The derivatives are related to the Sellmeier's equations for KDP since

$$\frac{dk}{d\omega} = \frac{n(\omega)}{c} + \frac{\omega}{c} \frac{dn}{d\omega} \quad (18)$$

so that the signal/idler angle Ω can be explicitly computed. These derivatives correspond to the group index for signal ($n_{gs} = ck_s/d\omega_s$) and idler ($n_{gi} = ck_i/d\omega_i$). Hence, Eq.17 can be interpreted as the request for signal group velocity to equal the projection of idler group velocity along the signal direction. Note that it is impossible to fulfill (17) if the group velocity of the idler is smaller than that of the signal. For the case under consideration ($\lambda_p = 349$ nm), this generalized matching condition can be achieved in the signal region between 400 and 700 nm. Fig.3 shows the signal group velocity as a function of $\lambda_s = 2\pi c/\omega_s$ (continuous line). The dashed line corresponds

to the idler velocity at $\omega_i = \omega_p - \omega_s$ versus the signal wavelength. Finally, it is possible to compute the (signal wavelength independent) angle α between the pump and the signal, which turns out to be

$$\sin \alpha = \frac{k_i}{k_p} \sin(\arccos [n_{gi}/n_{gs}]) \quad (19)$$

The FWHM bandwidth of the amplified signal versus λ_s for a KDP-based Type I amplifier operated in non-collinear geometry is shown in Fig. 4. As for Fig.1, the bandwidth has been computed assuming a pump wavelength of 349 nm and a pump intensity of 2 GW/cm². Again, the crystal length L for G=1000 is about 2 cm. Fig.5 shows the variation of the gain as a function of the wavenumber difference with respect to the central wavenumber ($1/\lambda_s$), which the angle α has been tuned for. The continuous line refers to $\lambda_s = 550$ nm (maximum bandwidth). The dotted and dashed lines refer to $\lambda_s = 450$ nm and $\lambda_s = 650$ nm, respectively. Figs.4 and 5 represent a key result: in non-collinear geometry the broadband window for the exploitation of the DPSSL or XeF drivers corresponds to a signal wavelength of about 550 nm. This region is accessible by a modelocked Ti:sapphire oscillators (signal generator) after self-phase modulation [28] and frequency doubling. It provides the seed signal (at the nJ level) that is amplified by the chain of low power amplifiers⁷. The pump signal for the low power amplifiers (<5 J) can be either derived by the main pump or, if necessary, by a dedicated low energy pump at a more appropriate wavelength. Finally, the signal is sent to the power amplifier operating in pump depletion mode. The studies performed in 2002 by I. Ross and coauthors [27] indicate that extraction efficiencies of the order of 40% can be obtained. In particular, a 4 kJ pump pulse would provide a broadband amplified signal of about 1.6 kJ. The actual light on target depends on the quality of the amplified signal and the compression optics and it is discussed in the next section.

4 Proton production and acceleration

The pulse duration that can be achieved after the amplification process is dominated, to first order, by the bandwidth of the seed signal and the gain bandwidth of the OPCPA even if additional effects connected to the beam quality entering the compressor and the compressor itself should be taken into account. In particular, the spectral phase [26, 27] generated in an optical parametric amplification when the seed signal is chirped plays a role in setting up the recompression system. For the case under study, the phase Φ of the amplified signal is given [26] by

$$\Phi = \text{atan} \left[\frac{B \sin(\Delta k/2L) \cosh B - (\Delta k/2L) \cos B \sinh B}{B \cos(\Delta k/2L) \cosh B + (\Delta k/2L) \sin(\Delta k/2L) \sinh B} \right] \quad (20)$$

⁷See e.g. Sec.3.1 of [12].

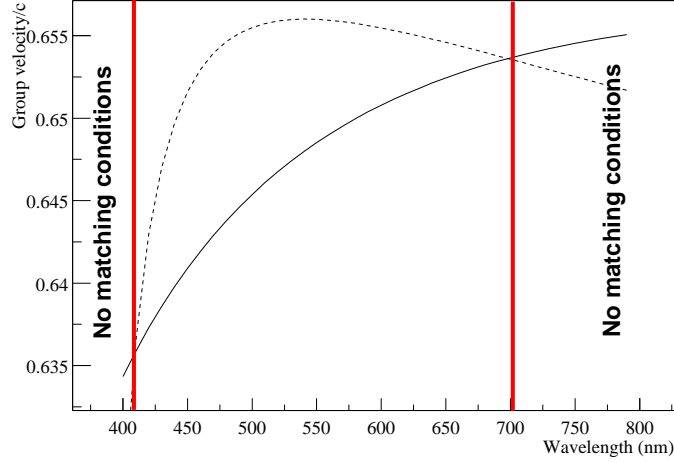


Figure 3: (Continuous line) Signal group velocity as a function of $\lambda_s = 2\pi c/\omega_s$. (Dashed line) Idler velocity at $\omega_i = \omega_p - \omega_s$ versus signal wavelength.

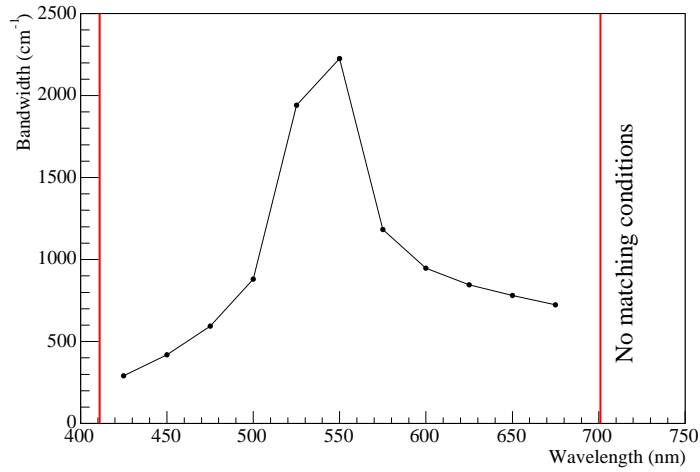


Figure 4: FWHM bandwidth expressed in wavenumbers ($1/\lambda$) versus signal wavelength for $\lambda_p = 349$ nm. The KDP-based amplifier ($G=1000$ at central wavelength) is operated in Type I non-collinear mode (see text for details).

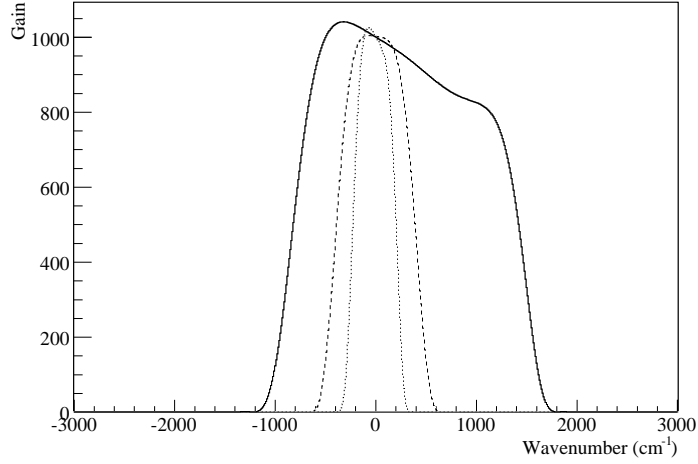


Figure 5: Gain versus the wavenumber difference with respect to the central wavenumber ($1/\lambda_s$), which the angle α has been tuned for. The continuous line refers to $\lambda_s = 550$ nm (maximum bandwidth). The dotted and dashed lines refer to $\lambda_s = 450$ nm and $\lambda_s = 650$ nm, respectively. The KDP-based amplifier ($G=1000$ at central wavelength) is operated in Type I non-collinear mode (see text for details) at $\lambda_p = 349$ nm.

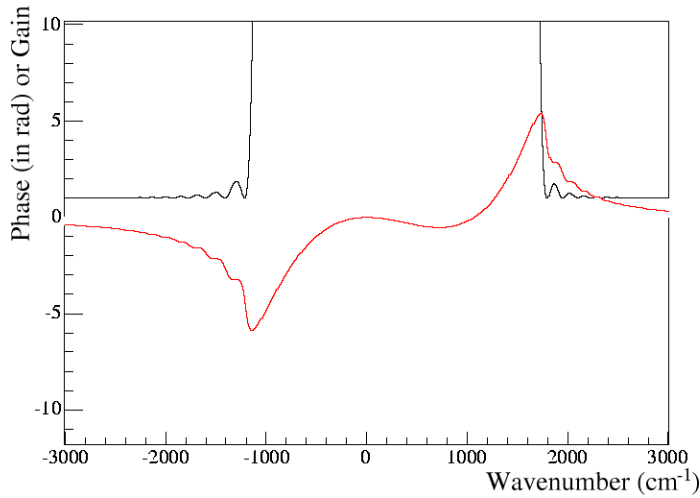


Figure 6: Phase of the amplified signal (light line) and gain (dark line) for the amplifier parameters of Fig.5 and $\lambda_s = 550$ nm.

and it is shown in Fig.6 (light line) for the amplifier parameters of Fig.5 and $\lambda_s = 550$ nm. For sake of clarity, the region where gain is > 1 (dark line) is also shown.

For this class of spectral chirping [27], nearly ideal recompression can be achieved as far as cubic phase terms can be compensated. Neglecting the throughput efficiency of the compressor and the losses due to the spectral clipping on the gratings, the output

power P for a Gaussian profile is:

$$P \simeq 1.6 \text{ kJ} \frac{\Delta\nu_{FWHM} \text{ (Hz)}}{0.44} = 240 \text{ PW} \quad (21)$$

if the bandwidth is dominated by the OPCPA gain bandwidth at $\lambda=550 \text{ nm}$ (2200 cm^{-1}). The actual maximum intensity on target depends on the quality of the optics and the available compressor gratings. Note, however, that operating near diffraction limit is not requested in the present case. It has been shown [7, 8] that RPD acceleration mechanism is fully operative for $I = 1 \times 10^{23} \text{ W/cm}^2$, although the transition region between the low intensity regimes and the RPD one is presently unexplored both from the experimental and from the numerical point of view. In the RPD case, the energy of the accelerated ions depends on the intensity and pulse duration according to Eq. (17) in Ref. [8]

$$\mathcal{E}_{p,kin} = m_p c^2 \frac{2w^2}{2w + 1} \quad (22)$$

while the number of accelerated ions depends solely on the illuminated area S [8]: $N_p = n_0 S l_0$. Here w is proportional to the laser pulse energy, \mathcal{E}_{tot} . It is given by $w = \mathcal{E}_{tot}/n_0 l_0 m_p c S$. The efficiency of the laser energy transformation into the fast proton energy is

$$\eta = \frac{N_p \mathcal{E}_{p,kin}}{\mathcal{E}_{tot}} = \frac{2w}{2w + 1}. \quad (23)$$

In the ultrarelativistic limit, $w \gg 1$, the efficiency tends to unity, and it is small in the nonrelativistic case when $w \ll 1$.

The studies performed in [7] made use of 27 fs (FWHM) gaussian pulses of $I = 1.4 \times 10^{23} \text{ W/cm}^2$ and, at these intensities, protons are accelerated following an $t^{1/3}$ asymptotic law up to kinetic energies of $\sim 30 \text{ GeV}$. These numerical studies are extremely challenging even for large parallel computer facilities. In order to reduce complexity, the study has been carried out with laser pulse of relatively small focal spot. In addition, the dynamical evolution has been followed up until the $t^{1/3}$ asymptotic behaviour is reached (i.e. before the complete laser-plasma decoupling). The overall laser energy to proton kinetic energy conversion efficiency at that time is 40%. Extrapolation up to the time of decoupling indicates that an energy conversion efficiency of 57% can be reached and the maximum kinetic energy for the above parameters exceeds 30 GeV. In the case under consideration, the illuminated area corresponding to an intensity on target of $I = 1.4 \times 10^{23} \text{ W/cm}^2$ is $S = 1.5 \times 10^{-10} \text{ m}^2$, i.e. a circular spot of 7 μm radius. Since the kinetic energy reached by the protons is proportional to the product of intensity and duration, a single shot (7 fs FWHM) would accelerate particles up to about 8 GeV. The number of accelerated protons N_p corresponds to the energy on target \mathcal{E}_{tot} corrected for the laser-to-ion energy transfer efficiency (η) divided by the proton kinetic energy ($\mathcal{E}_{p,kin}$).

$$N_p = \frac{\eta \mathcal{E}_{tot}}{\mathcal{E}_{p,kin}} \simeq 7 \times 10^{11} \text{ protons/pulse} \quad (24)$$

There is, however, an important caveat to be stressed. The RPD mechanism is fully operative if the illuminated area is sufficiently large so that border effects can be neglected [8]. Due to limited computational resource, a systematic study of the size and scaling of the border effect is not available at present. Results from [7] indicates that, at the intensities mentioned above, the border corona has a depth of the order of $5 \mu\text{m}$. This implies that either the beamlet arrangement should be able to illuminate uniformly a relatively large area, as it is done e.g. for the fuel target when the driver works in ICF mode, or that a significant higher energy should be used for the pump in a proper chain of KDP amplifiers. This energy is not used to increase the pump or the signal intensity but only the surface S , therefore it does not challenge the damage threshold of the amplifier/compressor components.

From Eq.24, it follows that a single ICF beamline operating at 10 Hz would be equivalent to a 10 kW proton driver. Clearly, a full ICF facility (2 MJ pump energy at a repetition rate of 10 Hz) would allow the construction of an extremely ambitious proton driver in the multi-MW intensity range (see Fig.7). Differently from traditional proton drivers, a laser driven device is highly modular, while for RF-based accelerators particles have to be stacked in a single lattice; in the RPD regime the stability conditions during acceleration are much less stringent than for traditional drivers since acceleration occurs nearly instantaneously and not in long periodical structures. Anyway, the possibility to develop laser fusion in strict connection with particle acceleration represents *per se* a fascinating research line.

5 Conclusions

If experimentally confirmed, the radiation-pressure dominated (RPD) acceleration mechanism [7] will offer a stable and efficient operation regime for laser-driven proton boosters. In particular, it has been emphasized [8] the opportunity to develop these facilities in conjunction with projects for inertial confinement fusion (ICF) and neutron spallation sources. In this paper, we have shown for the first time that the pulse compression requests to make operative the RPD regime do not fall in contradiction with the power requests of an ICF driver and we discussed explicitly one solution based on optical parametric chirped pulse amplification (OPCPA). Compatibility regions have been identified for OPCPA amplifiers based on Potassium Dihydrogen Phosphate operated in non collinear mode. In this configuration, bandwidths exceeding 2000 cm^{-1} (FWHM) have been obtained.

Acknowledgments

The authors would like to thank M. Borghesi and P. Migliozzi for insightful discussions and suggestions.

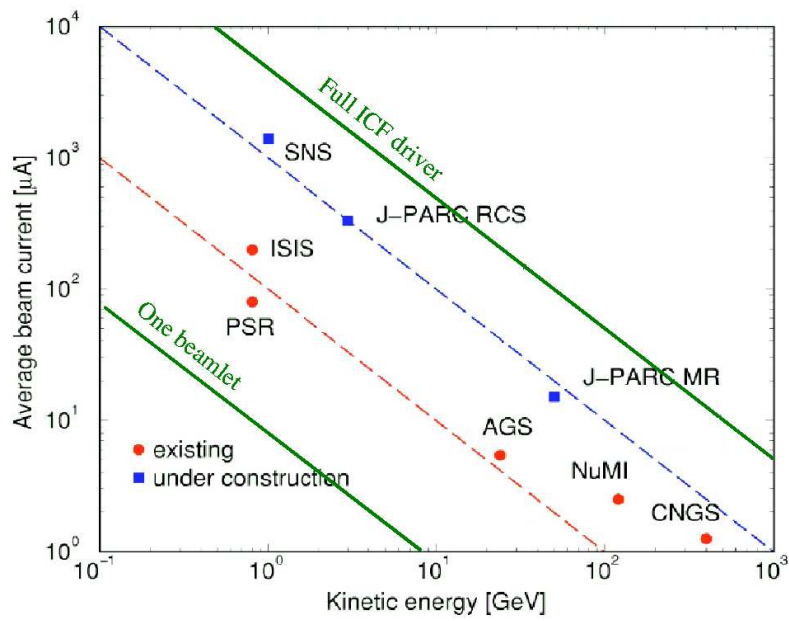


Figure 7: Average proton current versus proton kinetic energy for various existing facilities. The two green lines correspond to a driver obtained by a single 4 kJ beamlet and by the full ICF facility (2 MJ at 10 Hz rap.rate).

References

- [1] V. I. Veksler, in Proceedings of CERN Symposium on High Energy Accelerators and Pion Physics, Geneva, Vol.1, p.80, 1956; G.I. Budker, *Ibid*, p.68; Ya.B. Fainberg, *Ibid*. p.84.
- [2] K. Shimoda, *Appl. Optics* **1** (1962) 33.
- [3] T. Tajima, J.M. Dawson, *Phys. Rev. Lett.* **43** (1979) 267.
- [4] D. Strickland, G. Mourou, *Opt. Commun.* **56** (1985) 219.
- [5] A.V. Gurevich, L.V. Pariiskaya, L.P. Pitaevskii, *Sov. Phys. JETP* **22** (1965) 449 [*Zh. Eksp. Teor. Fiz.* **49** (1965) 647]; A.V. Gurevich, L.V. Pariiskaya, L.P. Pitaevskii, *Sov. Phys. JETP* **36** (1973) 274 [*Zh. Eksp. Teor. Fiz.* **63** (1972) 516]; S.J Gitomer *et al.*, *Phys. Fluids* **29** (1986) 2679.
- [6] For a recent review and references to the original papers see e.g. A. Maksimchuk *et al.*, *Plasma Phys. Rep.* **30** (2004) 473.
- [7] T.Zh. Esirkepov, M. Borghesi, S.V. Bulanov, G. Mourou, T. Tajima, *Phys. Rev. Lett.* **92** (2004) 175003.
- [8] S.V. Bulanov, T.Zh. Esirkepov, P. Migliozzi, F. Pegoraro, T. Tajima and F. Teranova, *Nucl. Instrum. Meth. A* **540** (2005) 25.
- [9] G. Mourou, T. Tajima, S.V. Bulanov, *Rev. Mod. Phys.* in press.
- [10] J.A. Paisner, J.D. Boyes, S.A. Kumpan, W.H. Lowdermilk, M. Sorem, *Laser Focus World* **30** (1994) 75.
- [11] A. Dubietis, G. Jonusauskas, A. Piskarskas, *Opt. Commun.* **88** (1992) 437.
- [12] I. Ross *et al.*, *Opt. Commun.* **144** (1997) 125.
- [13] R. Bieri *et al.*, *Fusion Technol.* **21**, (1992) 1583.
- [14] J.L. Emmett, W.F Krupke, *Sov. J. Quant. Electron.***13**, (1983) 1; W.F Krupke, *Fusion Technol.* **15** (1989) 377.
- [15] C. Bibeau *et al.*, “Diode Pumped Solid State Laser Driver for Inertial Fusion Energy”, Talk at 16th ANS Topical Meeting on the Technology for Fusion Energy, Madison, WI, 14-16 September 2004.
- [16] C. Bibeau *et al.*, Proceedings of the International Forum on Advanced High Power Lasers and Applications, UCRL-JC-133970, 1999.
- [17] J.D. Sethian *et al.*, *Proc. IEEE*, **92** (2004) 1403.

- [18] I.V. Sviatoslawky *et al.*, Fusion Technol. **21** (1992) 1470.
- [19] V.N. Smiley, in Proc. SPIE High Power Gas Laser, p.1225, 1990.
- [20] See e.g. J.J. Ewing, Optics and Photonics News, p.23, May 2003.
- [21] J.J. Ewin *et al.*, IEEE J. Quant. Electron., **15** (1979) 368.
- [22] I.N. Ross *et al.*, Laser Part. Beams **17** (1999) 331.
- [23] S.P. Velsko, W.F. Krupke, in “Nonlinear Frequency Generation and Conversion”, M.C. Gupta W.J. Kozlowsky, D.C. MacPherson eds., Proc. SPIE **2700** (1996) 6.
- [24] R.W. Boyd, “Nonlinear optics”, 2nd ed., Academic Press, 2003.
- [25] G. Cerullo, S. De Silvestri, Rev. Sci. Instrum. **74** (2003) 1.
- [26] J.A. Armstrong, N. Bloembergen, J. Ducuing, P.S. Pershan, Phys. Rev. **127** (1962) 1918.
- [27] I.N. Ross, P. Matousek, G.H.C. New, K. Osvay, J. Opt. Soc. Am. **B19** (2002) 2945.
- [28] A. Baltuska, Z. Wei, M.S. Pshenichnikov, D.A Wiersma, Optics Lett. **22** (1997) 102.